J. Phys. Chem. A **2006,** *110,* 9145−9152

Ab Initio Investigation of the $n \rightarrow \pi^*$ Transitions in Thiocarbonyl Dyes

Denis Jacquemin,* Valérie Wathelet,[†] and Eric A. Perpète[‡]

Laboratoire de Chimie Théorique Appliquée, Facultés Universitaires Notre-Dame de la Paix,
rue de Bruxelles, 61, B-5000 Namur, Belgium

Received: April 27, 2006; In Final Form: May 23, 2006

The $n \rightarrow \pi^*$ transitions in more than 100 thiocarbonyl dyes have been calculated with an ab initio procedure relying on the combination of time-dependent density functional theory (TD-DFT) for evaluating excited states and the polarizable continuum model (PCM) for modeling the bulk solvent effects on both the geometrical and electronic structures. Two hybrid functionals (B3LYP and PBE0) and several basis sets, some including f polarization functions, have been used. B3LYP provides the most accurate raw estimates, but once simple linear regression is performed, both functionals give similar results with a small advantage for PBE0. By use of the latter, the mean absolute deviation with respect to experiment is limited to 0.06 eV whereas less than 20% of the estimates differ from absorption data by more than 0.10 eV. To assess the validity limits of our model, compounds containing multiple C═S chromophores have also been considered.

I. Introduction

To classify organic dyes, one can either focus not only on their constituting chromophoric units (carbonyl, diazo, nitro, etc.), on the dyeing procedure (acid, basic, vat, disperse, etc.), or on their origin (mineral, vegetal, animal, etc.) but also on the electronic process involved in the color of the materials.[1] Using this latter criterion, one could first separate emitting and nonemitting compounds. Coumarins are prototypes of the first category: most of them absorb light in the near-UV domain and emit light by fluorescence in the visible region of the electromagnetic spectrum. However, most industrial dyes pertain to the second group, where the color appears due to the absorption of photons in the visible domain. Several nonemitting dyes present a strong dipole-allowed singlet $\pi \rightarrow \pi^*$ transition, but numerous compact molecules do not possess such a transition in the visible region and are colored due to $n \rightarrow \pi^*$ excitations, which imply smaller energies. According to Griffiths,[2] the three major $n \rightarrow \pi^*$ chromogens are diazo ($R_1{-}N{=}N{-}R_2$), nitroso ($R{-}N{=}O$), and thiocarbonyl ($R_{1,2}{-}C{=}S$, **I** in Figure 1). Most diazo dyes of practical interest are built on a diazo-benzene ($R_{1,2}{=}Ph$) skeleton in which strong $\pi \rightarrow \pi^*$ transitions mask the $n \rightarrow \pi^*$ contributions, except for the simplest structures. In the nitroso class, that we recently investigated,[3] the color mainly depends on the atom attached to the NO group. Thiocarbonyl dyes[4,5] present transitions covering almost the visible part of the electromagnetic spectrum (depending on R_1 and R_2) and are also highly “color-tunable”. Experimentally, the first systematic studies of the UV−vis spectra of these molecules began in the sixties with the works of Janssen,[6,7] Sandström,[8−12] and Korver et al.[13,14] Fabian, Mayer, and co-workers soon rationalized these absorption spectra by using a combination of measurements and semiempirical theoretical results.[15−17] More recently, experimental high-resolution analysis of the spectra of small gas-phase thiocarbonyl derivatives have been performed by Moule, Clouthier, and co-workers.[18−21]

This work aims at further investigating the wavelength of maximum absorption (λ_{max}) of a series of thiocarbonyl dyes by using ab initio quantum chemical approaches. Our purpose is the quantitative determination of the first absorption energy of thiocarbonyl derivatives. One of the major difficulties in predicting, with theoretical tools, the color of organic compounds is the astonishing biological accuracy of a standard human eye that can distinguish, in some parts of the visible spectrum, very small color shifts (less than 1 nm λ_{max} differences). Such an accuracy could only be (possibly) obtained for gas-phase molecules with highly correlated methods such as EOM-CC using high-order excitations and very extended basis sets,[22] which are completely out of computational reach. Indeed, these dyes possess numerous electrons and are used in diluted solutions or grafted on surfaces. In regards to practical industrial applications, the theoretical calculations shall be graded as serious competitors to experimental approaches for developing new dyes and/or pigments if they can deliver λ_{max} values within a 5 to 15 nm accuracy (~0.05 eV), which is still a tremendous challenge. That explains why empirical rules, similar to Woodward−Fieser’s, are still in use, to predict the color. For instance, additive procedures (i.e., group contributions) have successfully been designed for anthraquinones[23] and thiocarbonyls.[15] Though these rules are of practical interest, they are often nontransferable to other families of dyes and, more importantly, are limited by the experimental input. Indeed, they are unable to foresee the spectra of a given chromophore substituted by new auxochroms. To overcome this difficulty, one could lean toward semiempirical methods that often deliver useful chemical insights for hypothetical structures. Unfortunately, these approaches seem unable to consistently and quantitatively predict the λ_{max}. For instance, the popular ZINDO method nicely predicts the excitation energies in anthraquinone dyes[24] but, on the contrary, completely misses the target for indigoïds.[25,26] The main problem with semiempirical theories is that, contrary to ab initio approaches, it is very difficult to know beforehand when the predictions are likely to be reasonable or not. Such inconsistency is observed for thiocarbonyls. For instance, the ZINDO//AM1

---

* To whom correspondence should be addressed. E-mail: denis.jacquemin@fundp.ac.be. Homepage: http://perso.fundp.ac.be/~jacquemd. Research Associate of the Belgian National Fund for Scientific Research.

[†] E-mail: valerie.wathelet@fundp.ac.be.

[‡] E-mail: eric.perpete@fundp.ac.be. Research Associate of the Belgian National Fund for Scientific Research.

10.1021/jp062580d CCC: $33.50

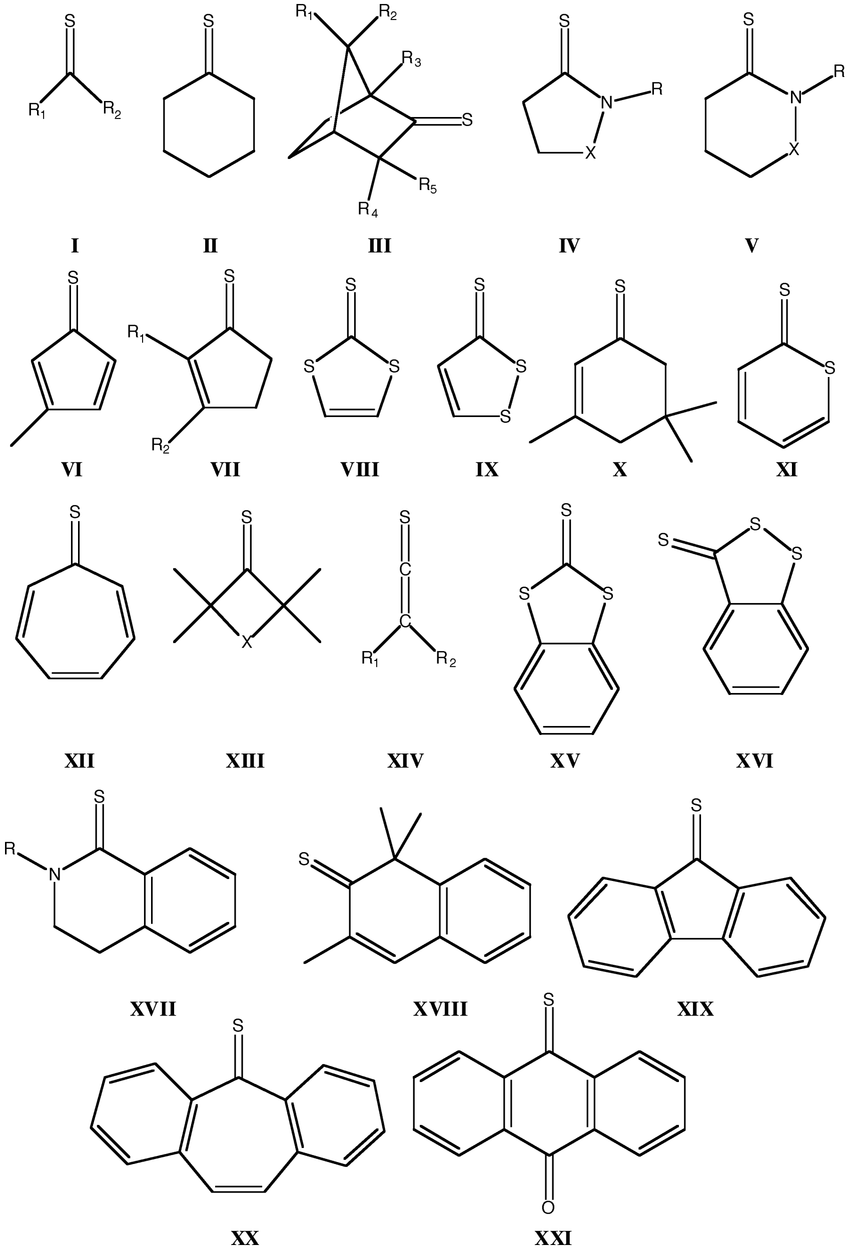

Figure 1. Sketch of the investigated compounds.

(gas-phase calculations) approach gives a very accurate $\lambda_{\max}$ of 507 nm (experimental value, 499 nm[16] in cyclohexane) for thioacetone ($Me_2C{=}S$), while for thiocarbonyl fluoride ($F_2C{=}S$), it predicts a 441 nm transition, 0.7 eV off the 352 nm measurement:[27] even in a given family of dyes, the accuracy level is inconsistent. For a large set of dyes, Adachi and Nakamura also obtained relatively poor correlations between experimental values and INDO/S or CNDO/S estimates.[28] Actually, the most promising scheme for systematically and routinely evaluating dyes' UV−vis spectra is the time-dependent density functional theory (TD-DFT).[29] Indeed, TD-DFT is often found robust and efficient for evaluating the low-lying excited spectra of conjugated molecules[30−33] and has been used for countless applications.[34−44] One important advantage of "conventional" TD-DFT (compared with semiempirical approaches) is that its main limitation is recognized: it tends to be inefficient for charge transfer dyes, for which the predicted ground-to-excited-state energy tends to be strongly undershot when the donor and acceptor groups are far apart.[45,46] This family of dyes set aside, one expects TD-DFT excited-state energies within a 0.4 eV prediction with respect to experiment (with hybrid functionals),[47] still far away from our 0.05 eV target. Though several specific TD-DFT studies can be found, only a couple are really comprehensive. The first is due to Guillaumont and Nakamura who obtained a mean absolute error (MAE) of 0.19 eV with B3LYP/6-31G, for a large panel of organic dyes.[48] The second is due to Fabian et al. who reported a B3LYP/6-31+G(d) MAE of 0.29 and 0.24 eV for $\pi \rightarrow \pi^*$ transitions in sulfur-free (SF) and sulfur-bearing (SB) molecules, respectively.[49] For $n \rightarrow \pi^*$ transitions that are often well localized, the MAEs tend to be smaller: 0.20 eV (SF)[49] and 0.09 eV (SB).[50,49] Though some of the SB molecules in refs 50 and 49 belong to the thiocarbonyl class, Petiau and Fabian specifically studied the C=S chromophore in a separate contribution[51] that is, to our knowledge, the only previous ab initio work on the subject with the studies of adiabatic transition in thioacetone[52] and thioformaldehyde.[53] For the 13 molecules for which a comparison with $n \rightarrow \pi^*$ measurements could be achieved, Fabian and Petiau deduced a 0.12 eV MAE.[51] The MAEs obtained for all these gas-phase TD-DFT computations using double-ζ basis sets are well above the required threshold for dye design. Once larger basis sets are selected and solvent effects explicitly included in the model,[54] the errors tend to be smaller. For instance, we obtained an MAE of 0.05 eV for nitroso derivatives,[3] 0.07 eV for diazonium salts,[43] 0.02 eV for indigo derivatives,[25] and 0.03 eV for thioindigoïds,[26] whereas da Silva and co-workers also report a nice theoretical/experimental match for six cationic dyes.[55] In all these latter investigations, the bulk solvent effects are taken into account for the computation of the absorption spectrum. Of course, as in any DFT investigation, the choice of an appropriate functional might be essential to attain such agreement. At this stage, it is not yet possible to determine unambiguously what is the most adequate functional for a given class of dyes, but it is clear that functionals containing between 20% and 25% of exact exchange generally provide, at least, satisfactory results.

In this paper, we extend the demonstration of the high predictive accuracy of TD-DFT to the first electronic transition of thiocarbonyl dyes, once extended basis sets are selected and bulk solvent effects are accounted. The *pros* and *cons* of the most widely used hybrids are discussed, as well as the role of f polarization functions.

II. Computational Details

All calculations have been performed with the Gaussian03 suite of programs.[56] Except when noted, default thresholds, procedures, and algorithms have been used. We have used a three-stage methodology: (1) the optimization of the ground-state structure, (2) the analytic determination of the vibrational spectrum, and (3) the evaluation of the electronic excited states. For all steps, we have used two hybrid functionals. On the one hand, the popular three-parameter B3LYP functional,[57] in which the exchange is a combination of 20% Hartree−Fock (HF) exchange, Slater functional, and Becke's generalized gradient approximation (GGA) correction,[58] whereas the correlation part combines local and Lee−Yang−Parr (LYP)[59] functionals. On the other hand, the parameter-free PBE0 hybrid functional (sometimes refereed to as PBE1PBE) that was independently and simultaneously designed by two groups[60,61] and is built on the Perdew−Burke−Ernzerhof pure functional,[62] in which the exchange is weighted (75% DFT/25% HF) according to theoretical considerations.[63] For all calculations, the self-consistent field (SCF) convergence criteria have been tightened to, at least, 10^{-9} au.

For each molecule, the ground-state structure has been determined setting a TIGHT threshold, which ensures that the residual mean square (RMS) forces are smaller than 1×10^{-5} au at the end of the minimization process. These optimizations have been performed using a large series of Pople's basis sets (see next section), and it eventually appears that 6-311G(2df,p) provides converged geometries. For several molecules of Figure 1, different conformations are possible, and we have performed several tests to assess the most stable positions of side groups. For instance, as Carey and co-workers, we have found that SMe groups are more stable in s-cis than in s-trans positions.[64] Nevertheless, for extended side groups, it is not computationally tractable to test all possibilities, and therefore, one cannot completely guarantee that the used geometries are actually global minima in these cases, although the optimized structures are, at least, very "reasonable" local minima.

The vibrational frequencies have been evaluated by the analytical determination of the Hessian matrix using exactly the same level of theory and basis set as in the first step.

The transition energies to the first three singlet excited states of each molecule have been computed by TD-DFT calculations. These calculations have been performed with the 6-311+G(2df,p) basis set which provides converged $\lambda_{\max}$ for the studied transitions (see section 3.1), that is, an addition of extra polarization or diffuse functions to 6-311+G(2df,p) is not expected to significantly affect the computed $\lambda_{\max}$. As detailed in the Introduction, the excitations responsible for the color of thiocarbonyls present a $n \rightarrow \pi^*$ character associated with a small oscillator force, and the reported $\lambda_{\max}$ always correspond to the transition energy to the first singlet excited state, except for molecules with multiple thiocarbonyl groups (see section 3.3). Indeed, in most cases, other transitions belong to the UV region.

At each stage, the bulk solvent effects are evaluated by means of the polarizable continuum model (PCM) (default IEF-PCM approach).[65] In the PCM, one divides the model into a solute part, the dye, surrounded by the solvent. The solvent is represented as a structureless material, characterized by its macroscopic properties (dielectric constant, molecular volume, etc.). In most cases, the PCM default parameters have been used but, for some dyes, switching on the *NoAddSph* option and/or using *Radii* = *UAKS* was found necessary to allow a proper convergence of the run. Most solvents used in the experiments, such as cyclohexane (Cyclo), benzene (Benz), dichloromethane (DCM), or chloroform (Chl) are found in the solvent list available for the PCM implementation in Gaussian03. Nevertheless, heptane (Hept) has been used instead of hexane (Hex) and other noncyclic hydrocarbons (HC). In several experiments, Sandström and co-workers measured the spectra in a solvent containing hydrocarbon(s), generally heptane, and a small amount (between 0.05% and 10%) of DCM. For these mixtures (Mix), the main component, heptane, has been used in the calculation. For (diethyl)ether (DEE), we have used an *Epsinf* of 1.82. The PCM returns valid solvent effects when no specific interactions (such as hydrogen bonds) link the solute and the solvent molecules, and this statement holds in this study. In this paper, we have selected the so-called nonequilibrium PCM solutions for the TD-DFT calculations.[54]

In the tables and figures, we have systematically used nanometers (nm) as this unit has the favor of most spectroscopists. However, the statistical analysis performed with the Statgraphics Plus 5.1. program[66] have been carried out using both nanometers and electronvolts. The electronvolt values have been obtained from their nanometer counterpart using: $\Delta E_{\max,\mathrm{eV}} = 1239.84/\lambda_{\max,\mathrm{nm}}$.

III. Results

A. Basis Set Study. As a test case, thioacetone (**I**, $R_{1,2}$ = Me in Figure 1) went through a full basis set (BS) study, to assess the atomic functions needed to obtain a converged $\lambda_{\max}$. Convergence does not only mean a quantitative agreement with a much larger basis set (as such a match might originate from random factors), but also implies that further extension of the basis set, obtained by adding extra individual diffuse or polarization functions does not significantly affect the results. This theoretical investigation has been performed with the PBE0 hybrid functional in the gas phase. It is expected that the basis set effects would be similar when using the B3LYP functional. Thioacetone has been chosen for its small size which allows the use of very extended basis sets. As the chromophoric unit, C═S, does not include the side groups, it is reasonable to expect that $R_{1,2}$ substitutions will not affect the requested theoretical level.

The results are displayed in Table 1. Once at least one set of polarization functions is included, the BS effects for the geometry and UV−vis spectrum are almost independent of each

TABLE 1: Basis Set Study for the λ_{max} of Thioacetone, that is, I with $R_1 = R_2 = Me$[a]

	geometry					
UV−vis	6-31G	6-31G(d,p)	6-31+G(d,p)	6-311G(d,p)	6-311+G(d,p)	6-311G(2d,p)
6-31G	484	461	461	460	460	456
6-31G(d,p)	498	475	475	473	473	472
6-31+G(d,p)	502	479	479	478	478	476
6-311G(d,p)	495	473	473	472	472	470
6-311+G(d,p)	501	478	479	477	477	475
6-311+G(2d,p)	505	483	483	481	482	480
6-311+G(2df,p)	504	482	483	481	481	480
6-311++G(d,p)	501	478	479	477	477	476
6-311++G(2d,2p)	505	483	483	481	481	480
6-311++G(2df,2pd)	504	482	482	481	481	479
6-311++G(3df,3pd)	504	483	483	481	481	480
cc-pVTZ	503	481	481	479	479	478
aug-cc-pVTZ	504	482	482	480	480	479

	geometry					
UV−vis	6-311G(2df,p)	6-311++G(2d,2p)	6-311++G(2df,2pd)	6-311++G(3df,3pd)	cc-pVTZ	aug-cc-pVTZ
6-31G	457	458	457	456	458	458
6-31G(d,p)	471	472	471	470	472	472
6-31+G(d,p)	475	476	475	474	476	476
6-311G(d,p)	469	470	469	468	470	470
6-311+G(d,p)	474	475	474	473	475	475
6-311+G(2d,p)	479	480	479	478	480	480
6-311+G(2df,p)	478	479	478	478	479	479
6-311++G(d,p)	474	475	474	473	475	475
6-311++G(2d,2p)	479	480	479	478	480	480
6-311++G(2df,2pd)	478	479	478	477	479	479
6-311++G(3df,3pd)	479	480	479	478	480	480
cc-pVTZ	477	478	476	476	477	478
aug-cc-pVTZ	478	479	478	477	479	479

[a] All calculations have been performed in vacuo with the hybrid PBE0 functional.

other. For instance, the shift when using 6-31+G(d,p) instead of 6-31G(d,p) for the absorption spectra is always +4 or +5 nm, regardless of the geometry selected. Likewise, upgrading ground-state geometries from 6-31G(d,p) to 6-311G(2d,2p) leads to a −2 to −3 nm displacement of the λ_{max} for all absorption spectra. As foreseen,[51] the BS unequally affects the absorption spectrum and the geometry: adding diffuse functions to 6-31G(d,p) has a negligible (large) effect on the geometry (absorption spectrum). From Table 1, it is obvious that one set of polarization functions is always required whereas diffuse functions are mandatory for the electronic spectra. Consequently, the 6-31+G(d,p) basis set, chosen by Petiau and Fabian,[51] features the most important functions. Indeed, it gives a λ_{max} in very good agreement with much larger basis sets, and it even provides exactly the same λ_{max} as the aug-cc-pVTZ result (479 nm). However, if one carefully examines the evolution of the λ_{max} with respect to the extension of the basis set used for the geometry optimization, one notes that the third valence functions, the second set of d polarization, and the first set of f orbitals lead to small but systematic changes in the computed spectrum. Therefore, 6-311G(2df,p) can be considered as perfectly suitable for geometry optimizations, as adding extra polarization/diffuse functions leaves λ_{max} almost unchanged (typical variations ±1 nm). For the absorption spectra, the double/triple-ζ shift is small (−1 nm), but the addition of diffuse functions on second and third row atoms produces a +5 nm shift. Likewise, a second set of d polarization orbitals is also mandatory (+5 nm) whereas diffuse functions on the hydrogen atoms have almost no impact. Therefore, 6-31+G(2d,p) could probably be viewed as a valuable accuracy/size choice for the TD-DFT step. Nevertheless, it might look weird to use a smaller basis set for the excited states than for the ground-state geometry. Therefore, we have used 6-311+G(2df,p) during TD-DFT calculations. This combination of basis sets [6-311+G(2df,p)//6-311G(2df,p)] is refereed to as **BS-II** in the following. We have also used a less demanding approach [**BS-I** = 6-311+G(2d,p)//6-311G(d,p)] to (statistically) assess the importance of extra polarization.

B. Comparisons and Discussion. In Table 2, we compare theoretical and experimental λ_{max} for the $n \rightarrow \pi^*$ transition in more than 100 thiocarbonyls featuring a large panel of side groups: amino, methoxy, halogens, cyano, and so forth, and therefore, constituting a very broad set of chemicals. Large (conjugated) compounds have been considered as well (see Figure 1). The experimental values have been chosen following five criteria: (1) no data reported prior to 1960 has been used because very old data tend to be less accurate for such $n \rightarrow \pi^*$ transitions, (2) only absorption spectra have been accepted, that is, adiabatic measurements were discarded, (3) as long as possible, λ_{max} values obtained in aprotic media have been selected, as specific interactions are not included in the PCM model, (4) the dyes contain only one C═S chromophoric unit (multiple C═S molecules are considered in section 3.3), and (5) when multiple peaks are reported, that is, when the experimental spectra present a clear vibrational structure, we have used the absorption with the largest (experimental) transition probability. Despite these tight criteria, the measurements reported in Table 2 should not be viewed as error-free, as some could correspond to shoulders that are sometimes difficult to accurately resolve. For thiocarbonyl chloride ($Cl_2C{=}S$), although the $n \rightarrow \pi^*$ appears as a well-separated transition, it is has been shown that deconvoluting the spectrum still leads to an 8 nm displacement of the λ_{max} value.[67] Some experimental values also appear doubtful in regards to other measurements. For instance, it looks questionable that replacing a Me by a Pr segment in Me-CS−SMe provokes a +42 nm shift, if changing both Me of thioacetone by Pr leads to a +4-nm-only variation. The value Pr−CS−SMe is obviously too large, as can also be concluded by examining

TABLE 2: Comparison between Theoretical and Experimental λ_{max} for the $n \rightarrow \pi^*$ Transitions in the Thiocarbonyls Dyes Sketched in Figure 1[a]

		PBE0		B3LYP			
molecule	solvent	**BS-I**	**BS-II**	**BS-I**	**BS-II**	exp	ref
I, $R_{1,2} = F$	gas	333	330	345	342	352	27
$R_{1,2} = Cl$	Hex	445	444	453	451	480^{b}	67
$R_{1,2} = Br$	gas	466	466	472	471	480	69
$R_1 = Cl, R_2 = Br$	gas	456	456	463	462	470	69
$R_{1,2} = Me$	Cyclo	474	471	486	482	499	16
$R_{1,2} = Pr$	Cyclo	467	464	479	476	503	70
$R_{1,2} = t\text{-}Bu^{d}$	Cyclo	512	510	526	523	540	71
$R_1 = CH{=}CH_2, R_2 = H$	Mat.^{c}	587	583	604	600	580	72
$R_{1,2} = CF_3$	Cyclo	573	567	585	579	580	73
$R_1 = CF_2Cl, R_2 = Cl$	Cyclo^{d}	490	487	502	499	510	73
$R_1 = CF_2Cl, R_2 = F$	Cyclo^{d}	412	409	427	423	425	73
$R_1 = CF_2Cl, R_2 = Ph$	Cyclo	585	582	603	603	*518*	73
$R_1 = Me$, $R_2 =$ cyclohexane	Cyclo	474	471	486	483	508	70
$R_1 = Me, R_2 = Cl$	Cyclo	446	445	453	452	437	15
$R_1 = NH_2, R_2 = CN$	DCM	424	422	442	439	438	8
$R_1 = NH_2, R_2 = CONMe_2$	DCM	353	352	364	362	375	8
$R_1 = NH_2, R_2 = Me$	Hept	352	352	365	364	367	9,10
$R_{1,2} = NH_2$	DEE	272	271	284	282	290(s)	6
$R_1 = NH_2, R_2 = NMe_2$	DEE	274	273	286	284	295(s)	6
$R_1 = NH_2, R_2 = OMe$	Hept	286	285	298	296	295	10
$R_1 = NH_2, R_2 = Ph$	Hept	408	407	424	423	418	9
$R_1 = NH_2, R_2 = SMe$	HC	333	332	344	343	357	6
$R_1 = NHCOMe, R_2 = Me$	Hept	407	405	423	421	425	10
$R_1 = NHCOMe, R_2 = NMe_2$	Hept	333	332	348	347	338	10
$R_1 = NHCOMe, R_2 = OMe$	Chl	324	323	338	336	333	10
$R_1 = NHCOMe, R_2 = SMe$	Chl	381	380	396	395	397	10
$R_1 = NMeCOMe, R_2 = OMe$	Chl	339	336	355	352	345	10
$R_1 = NMeCOMe, R_2 = SMe$	CHl^{d,e}	392	393	408	407	410	10
$R_1 = NHMe, R_2 = CONH_2$	DCM	399	399	417	416	399	8
$R_1 = NHMe, R_2 = CONHMe$	Mix	396	396	414	413	400	8
$R_1 = NHMe, R_2 = Me$	HC	349	348	362	360	360	6,12
$R_1 = NHMe, R_2 = NMe_2$	Cyclo	280	278	292	290	295(s)	6
$R_1 = NHMe, R_2 = OMe$	Hept	282	281	294	292	285(s)	11
$R_1 = NHMe, R_2 = Ph$	Hept	396	395	411	409	402	9
$R_1 = NHMe, R_2 = SMe$	hc	327	327	339	339	343	6
$R_1 = NMe_2, R_2 = Cl$	Cyclo	336	336	344	344	352	15
$R_1 = NMe_2, R_2 = CN$	Hept	430	427	448	445	433	8
$R_1 = NMe_2, R_2 = CONH_2$	DCM	359	355	369	366	370(s)	8
$R_1 = NMe_2, R_2 = CONHMe$	Mix	394	392	406	401	391	8
$R_1 = NMe_2, R_2 = CONMe_2$	DCM	345	344	357	355	359	8
$R_1 = NMe_2, R_2 = Me$	HC	348	347	361	359	365	6,12
$R_{1,2} = NMe_2$	HC	319	315	334	330	330	6
$R_1 = NMe_2, R_2 = OMe$	HC	283	282	295	292	286(s)	6
$R_1 = NMe_2, R_2 = Ph$	Hept	385	382	397	394	395	9
$R_1 = NMe_2, R_2 = SMe$	HC	327	327	339	339	343	6
$R_1 = NHPh, R_2 = CN$	Cyclo	453	452	472	470	448	15
$R_1 = NHPh, R_2 = Me$	Cyclo	372	373	386	386	394(s)	15
$R_1 = OEt, R_2 = Cl$	Cyclo	351	350	359	359	369	15
$R_1 = OEt, R_2 = Me$	Cyclo	358	357	370	368	377	7
$R_{1,2} = OEt$	Cyclo	293	292	304	302	303	7
$R_1 = OEt, R_2 = SEt$	HC	338	338	349	348	357	7
$R_1 = SCF_3, R_2 = Cl$	Cyclo^{d}	430	430	436	436	468	73
$R_1 = SCF_3, R_2 = F$	Cyclo^{d}	367	367	378	376	394	73
$R_1 = SCF_3, R_2 = CF_3$	Cyclo^{d,e}	498	497	509	507	532	73
$R_{1,2} = SCF_3$	Cyclo^{d,e}	457	456	469	468	497	73
$R_1 = SEt, R_2 = Me$	Cyclo	437	436	449	448	460	7
$R_1 = SEt, R_2 = CF_3$	Cyclo	471	468	485	482	494	74
$R_1 = SEt, R_2 = C_3F_7$	Cyclo	480	478	495	494	505	74
$R_{1,2} = SEt$	Cyclo	407	407	419	419	432	7
$R_1 = SMe, R_2 = CN$	^{f}	525	522	542	538	530	75
$R_1 = SMe, R_2 = Me$	Cyclo^{d}	434	433	446	445	456	16
$R_1 = SMe, R_2 = Pr$	Cyclo	434	433	447	445	*498*	74
$R_1 = SMe, R_2 = C_2F_5$	Cyclo^{d,e}	475	473	490	487	497	74
$R_{1,2} = SMe$	Cyclo	402	403	414	414	429	7,16
$R_1 = Ph, R_2 = H$	Mat.^{c}	579	577	597	594	575	72
$R_1 = Ph, R_2 = Me$	Cyclo	559	557	578	576	573	16
$R_1 = Ph, R_2 = t\text{-}Bu$	Benz	537	533	550	545	560	76
$R_{1,2} = Ph$	Cyclo	576	574	594	591	610,609	16,13
$R_1 = Ph, R_2 = SMe$	Cyclo	479	479	493	491	504	16
II	Cyclo	479	477	491	488	504	7
III, $R_{1,2,3,4,5} = H$	Benz	472	470	484	481	497	76
$R_{1,2,3} = Me, R_{4,5} = H$	Cyclo	472	470	483	481	493	7
$R_{1,2,3} = H, R_{4,5} = Me$	Benz	471	468	483	480	494	76
$R_{1,2} = H, R_{3,4,5} = Me$	Hex	468	466	481	478	488	7
$R_{1,2,3,4,5} = Me$	Benz	468	466	481	478	490	76
IV, $R = H, X = CH_2$	Mix	342	340	353	351	335	12
$R = Me, X = CH_2$	Mix	337	336	349	348	348	12
$R = H, X = CO$	Mix	387	386	401	399	399	12
$R = Me, X = CO$	Hept	385	384	400	398	395	12
V, $R = H, X = CH_2$	Mix	346	345	360	358	340	12
$R = Me, X = CH_2$	Hept	348	347	362	361	362	12
$R = H, X = CO$	Mix	404	402	419	417	417	12
$R = Me, X = CO$	Mix	415	413	431	429	424	12
VI	Mat (77k)^{c}	747	743	764	759	750	77
VII, $R_1 = H, R_2 = Me$	Cyclo	513	511	531	529	542	78
$R_1 = R_2 = Me$	Cyclo	507	505	524	522	529	78
VIII	Cyclo	408	410	421	422	428	16
IX	Cyclo	464	464	483	483	498	16,17
X	Cyclo	534	532	552	549	572	78
XI	Cyclo	495	495	520	520	587	16
XII	Cyclo	540	538	563	561	610	79
XIII,^{d} $X = CO$	Hex	509	506	520	517	520	80
$X = CH_2$	Hex	485	482	494	491	500	81
$X = S$	Hex	473	472	484	480	489	81
XIV, $R_1 = R_2 = tBu$	Cyclo	534	529	541	536	570	82
$R_1 = R_2 = CF_3$	Liq^{g}	472	468	481	477	503	83
XV	Cyclo	411	413	422	424	440	16
XVI	Cyclo	468	469	486	486	502	16
XVII, $R = H$	Hept	418	418	438	437	412	11
$R = Me$	Hept	422	421	442	440	425	11
XVIII^{d}	Cyclo	581	578	606	603	618	84
XIX	Cyclo	639	628	659	656	700	16
XX^{d}	Cyclo	562	559	578	574	605	16
XXI^{d}	CHl	687	691	716	718	697	85

[a] All values are in nanometers. (s) indicates that the peaks are reported as shoulders in the original experimental paper. Experimental values in italics are not used in theory/experiment comparisons (see text for more details). [b] Nonresolved spectrum, resolved spectrum: 488 nm. [c] Inert matrix measurements. Gas-phase calculations. [d] For some or all parts of the calculations, the *Noaddsph* has been switched on. [e] For some or all parts of the calculations, the *Radii = UAKS* option has been used. [f] Unspecified medium. Gas-phase calculations. [g] Pure liquid measurements. Gas-phase calculations.

similar perfluoro derivatives. The 518 nm figure for Ph−CS−CF$_2$Cl is also inconsistent. It corresponds to a −55 nm hypsochromic shift from for Ph−CS−Me whereas perhalogenation of alkyl side groups are always associated with significant bathochromic shifts: +81 nm from Me−CS−Me to CF$_3$−CS−CF$_3$, +34 nm from Me−CS−SEt to CF$_3$−CS−SEt, and +47 nm from Me−CS−Cl to CF$_2$Cl−CS−Cl. Consequently, these two compounds have been left aside and the following statistical analysis is based on the 102 “remaining” dyes.

In this study, all calculations have been performed with the explicit consideration of solvent effects, which can be quantified by comparing results with and without PCM terms included. For instance, with B3LYP/**BS-II**, the λ_{max} of thiocarbonyl chloride, $Cl_2C{=}S$, in heptane is 451 nm with a PCM//PCM, 451 nm with PCM//gas, 454 nm with gas//PCM, and 453 nm with gas//gas approaches. Therefore, one could believe that including the medium effect is unnecessary for thiocarbonyl derivatives. However, the B3LYP/**BS-II** λ_{max} values for thiourea, $(NH_2)_2C{=}S$, in DEE are 282, 294, 306, and 316 nm, for PCM//PCM, PCM//gas, gas//PCM, and gas//gas schemes, respectively. The changes between the PCM//PCM and gas//gas results correspond to 0.47 eV differences, which obviously cannot be neglected. In the case of thiourea, there is a change in the geometry when bulk solvent effects are considered: the amino groups are planar in DEE but nonplanar in the gas phase, and it tunes λ_{max}. Indeed, by forcing the planarity, one obtains 303 nm for the gas//gas calculation. This highlights the importance of having accurate geometries before performing any comparison with experimental

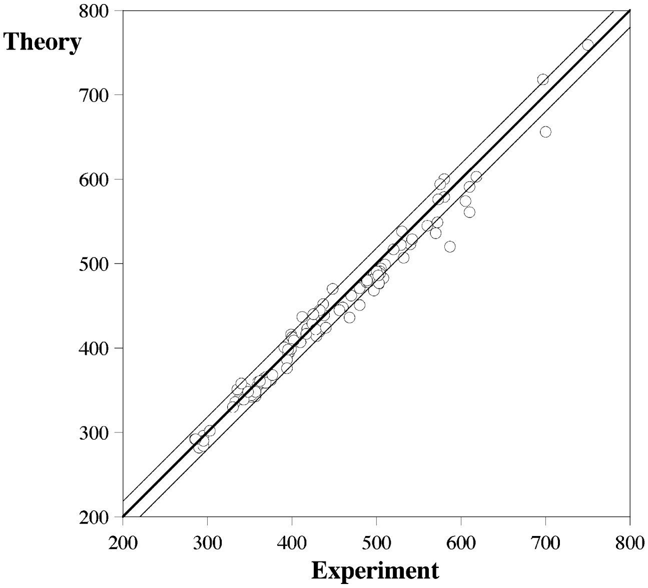

Figure 2. Comparison between experimental and theoretical (B3LYP, **BS-II**) $n \rightarrow \pi^*$ λ_{max}. All values are in nanometers. The central line indicates the perfect match, whereas side lines define borders for ±20 nm displacements.

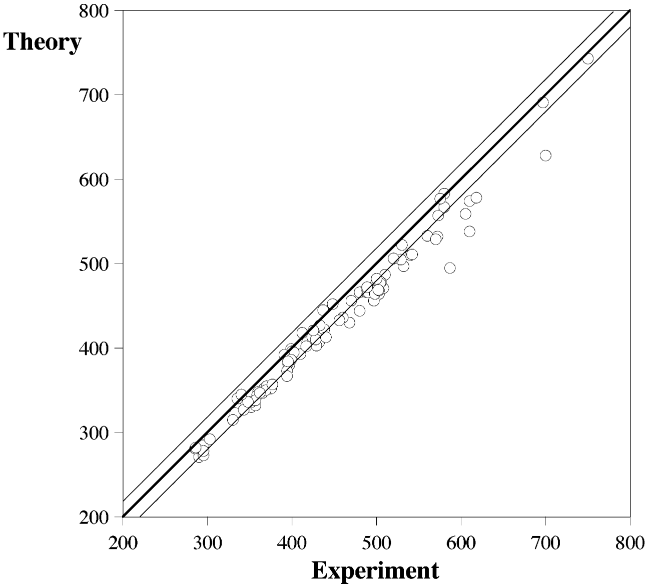

Figure 3. Comparison between experimental and theoretical (PBE0, **BS-II**) $n \rightarrow \pi^*$ λ_{max}. See Figure 2 for more details.

data. For the record, the λ_{max} value of $Cl_2C{=}S$ computed with PCM-B3LYP/**BS-II** on a gas-phase AM1 structure is 417 nm, far away from the figures computed with DFT ground states.

In Table 2, it is striking that the PBE0 excitation energies are systematically larger than their B3LYP counterparts, with an average λ_{max} difference of 13.4 nm (−0.094 eV) with **BS-II**. Upgrading **BS-I** to **BS-II** scheme leads, in most cases, to a small hypsochromic shift for both B3LYP and PBE0. Indeed the mean λ_{max} changes are −1.5 nm (0.010 eV) and −2.1 nm (0.014 eV), for Becke's and Adamo's functionals, respectively. Therefore, the inclusion of f atomic orbitals in the basis set has no impact on the results.

By using **BS-II**, which provides fully converged results, mean signed errors (MSEs) of −6.8 nm (0.034 eV) and −20.1 nm (0.129 eV) have been obtained for B3LYP and PBE0, respectively. The theory underestimates the λ_{max} (overestimates the excitation energies), especially with PBE0. The corresponding absolute errors (MAEs), favored in functional comparisons, are 12.6 nm (0.074 eV) for B3LYP and 20.8 nm (0.134 eV) for PBE0. Consequently, B3LYP is the functional of choice for evaluating the $n \rightarrow \pi^*$ λ_{max} of thiocarbonyls, as this 0.074 eV MAE appears much smaller than the standard errors reported by most TD-DFT investigations (see Introduction) and more specifically, significantly more accurate than the 0.12 eV MAE given by Petiau and Fabian for a 13 molecule set.[51] This difference probably originates in the explicit consideration of bulk solvent effect in our methodology, as BS effects are rather weak. Through the use of B3LYP/**BS-II**, the λ_{max} estimates are almost as accurate as the first-order additive rules designed by Fabian, Viola, and Mayer, although the latter was completely empirically tailored.[15] Theoretical and experimental λ_{max} are compared in Figure 2 (B3LYP) and Figure 3 (PBE0) with a nice agreement for the former with most cases presenting errors smaller than 20 nm. The corresponding ΔE_{max} figures in electronvolts are provided as Supporting Information. The largest B3LYP errors (in eV) appear for **XI** (0.272 eV), Cl−CS−SCF_3 (0.194 eV), and **V**, R = H, X = CH_2 (0.183 eV). By selecting the less demanding **BS-I**, we reach slightly smaller MAEs than with **BS−II**: 12.1 nm (0.073 eV) and 19.5 nm (0.125 eV), with B3LYP and PBE0 functionals, respectively. This could be regarded as positive from the common sense (faster calculations, results closer to experiment) point of view but quite disappointing from the quantum chemist point of view (converged results, less accurate prediction). In fact, this is due to, on the one hand, the bathochromic shift observed when removing f atomic orbitals and, on the other hand, the fact that TD-DFT λ_{max} values tend to be too small, that is, there is basis set/functional error compensation.

To estimate the correlation between theory and experiment, one can use simple linear regression (SLR). We have performed the fitting in both electronvolts and nanometer scales, using **BS-I** and **BS-II** basis sets combined with B3LYP and PBE0. The best correlation with experimental value is obtained with PBE0/**BS-II**

$$\lambda_{max,nm} = -4.690 + 1.058\lambda_{max,nm}^{PBE0-\mathbf{BS-II}} \quad (1)$$

$$\Delta E_{max,eV} = -0.042 + 0.971\Delta E_{max,eV}^{PBE0-\mathbf{BS-II}} \quad (2)$$

Using these equations, the MAEs are limited to 9.9 nm and 0.058 eV, respectively, whereas the adjusted correlation coefficients, R^2_{adj}, are 97.7% and 98.4%, respectively. These values are smaller by 2.2 nm and 0.015 eV than the most accurate unfitted approach (B3LYP/**BS-I**). Also, using eq 2, only 19.6% (20 out of 102) of the theoretical estimates differ from the experiment by more than 0.100 eV [6.9% (7 out of 102) by more than 0.150 eV]. With the raw B3LYP/**BS-II** results, the corresponding figures are 25.4% (26 out of 102) [9.8% (10 out of 102)], that is, the extreme deviations have also been reduced by the statistical treatment. The standard deviations, d_R, measuring the predictive accuracy of a statistical model, are 14.8 nm and 0.079 eV, for eqs 1 and 2, respectively. That means that the λ_{max} of thiocarbonyl dyes not included in our set can also be determined accurately: that is, $\lambda_{max}^{theo} = \lambda_{max}^{exp} \pm 14.8$ nm (or $\Delta E_{max,eV}^{theo} = \Delta E_{max,eV}^{exp} \pm 0.078$ eV). The results computed with eq 1 are displayed in Figure 4, whereas the ΔE_{max} computed with eq 2 can be found in the Supporting Information.

The SLR-B3LYP/**BS-II** equations are

$$\lambda_{max,nm} = -9.025 + 1.036\lambda_{max,nm}^{B3LYP-\mathbf{BS-II}} \quad (3)$$

$$\Delta E_{max,eV} = -0.083 + 1.018\Delta E_{max,eV}^{B3LYP-\mathbf{BS-II}} \quad (4)$$

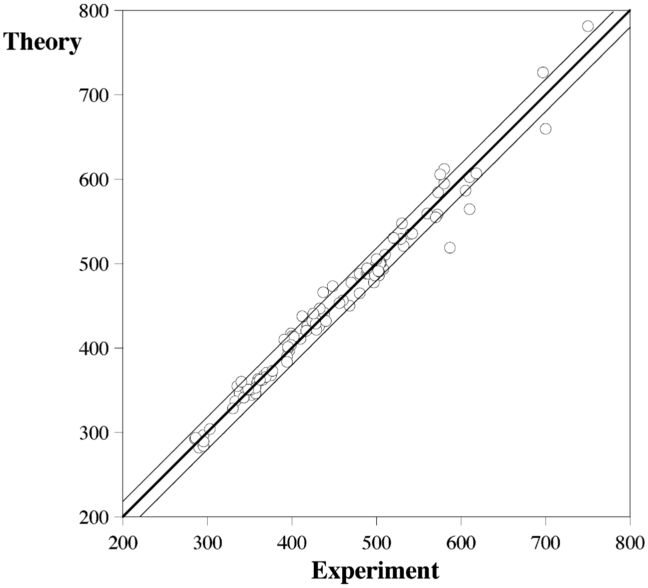

Figure 4. Comparison between the $\lambda_{\max}$ obtained, experimentally and by eq 1. All values are in nanometers.

TABLE 3: Theoretical (BS-II) and Experimental $\lambda_{\max}$ for Dyes with Multiple Thiocarbonyl Groups

molecule	solvent	PBE0	B3LYP	exp	ref
I $R_1 = NHMe$, $R_2 = CSNH_2$	Mix	482	508	486	8
$R_1 = NHMe$, $R_2 = CSNHMe$	Mix	468	494	462	8
$R_1 = NMe_2$, $R_2{=}CSNMe_2$	Mix	382	391	365	8
IV, R = H, X = CS	Mix	438/401	456/417	406	12
R = Me, X = CS	Hept	439/401	458/419	410/395	12
V, R = H, X = CS	Mix	464/421	484/439	476/427	12
R = Me, X = CS	Mix	495/430	517/449	500(s)/443/423	12
XIII, X = CS	Hex	516/493	531/491	500	80

[a] All values are in nanometers.

with an MAE of 10.6 nm (0.064 eV) and a d_R value of 14.9 nm (0.084 eV). Therefore, once statistically corrected, B3LYP and PBE0 provide almost the same accuracy for the $n \rightarrow \pi^*$ transition in thiocarbonyl dyes. Through the use of the smaller basis set combination, the resulting equations are

$$\lambda_{\max,\mathrm{nm}} = -3.339 + 1.051\lambda_{\max,\mathrm{nm}}^{\mathrm{PBE0-\mathbf{BS-I}}} \quad (5)$$

$$\lambda_{\max,\mathrm{nm}} = -8.929 + 1.031\lambda_{\max,\mathrm{nm}}^{\mathrm{B3LYP-\mathbf{BS-I}}} \quad (6)$$

$$\Delta E_{\max,\mathrm{eV}} = -0.040 + 0.974\Delta E_{\max,\mathrm{eV}}^{\mathrm{PBE0-\mathbf{BS-I}}} \quad (7)$$

$$\Delta E_{\max,\mathrm{eV}} = -0.093 + 1.025\Delta E_{\max,\mathrm{eV}}^{\mathrm{B3LYP-\mathbf{BS-I}}} \quad (8)$$

and provide MAEs of 10.0 nm (0.060 eV) with PBE0 and of 10.8 nm (0.066 eV) with B3LYP. That is only very slightly above the results obtained with the larger basis sets, indicating again that the inclusion of f orbitals is not mandatory for evaluating spectra of thiocarbonyl chromogens. To minimize the MAE and d_R, we combined of B3LYP and PBE0 results through a multiple linear regression (MLR) approach, similar to that successfully used for anthraquinone-based dyes.[68] However, this procedure did not bring any significant improvement over the SLR approach.

C. Polythiocarbonyl Dyes. In Table 3, we compare TD-DFT results and measurements for dyes presenting two C═S groups. For the derivatives of **I**, we find only one peak in the same region as the experiment (the next transition takes place at significantly higher energies) and we obtain a correct qualitative ordering of the three compounds, combined to a quantitative agreement. For **IV** and **V**, Berg and Sandström reported one, two, or three transitions depending on the molecule (and also on the solvent),[12] whereas we always found two $n \rightarrow \pi^*$ transitions. Having a close look to the shift between the different transitions in a given molecule, one obtains an experimental variation of 15 nm for **IV** (R = Me) that weakly reproduces our 39 nm theoretical shift. For **V**, the theoretical and experimental shifts are in good agreement (45 vs 49 nm for R = H, 68 vs 57 nm for R = Me). For **XIII**, we also obtained two transitions bracketing the single experimental peak. Though it did not show to be as efficient as awaited, our model still managed to yield qualitative predictions in the difficult case of dichromogenic species.

IV. Conclusions

The absorption spectra of 102 thiocarbonyl dyes, and more specifically the $n \rightarrow \pi^*$ transitions, have been computed with a PCM-TD-DFT approach using two hybrid functionals (B3LYP and PBE0) and two basis sets combinations. The present study points out that, if no fitting procedure is performed, B3LYP has an advantage on PBE0 for evaluating the $\lambda_{\max}$ of thiocarbonyls. Simple linear regressions have been performed and equations that minimize the theory/experiment discrepancies have been produced. Using such a procedure, the difference between the results of B3LYP and PBE0 are negligible. Our best model yields a MAE of 9.9 nm or 0.058 eV with less than 20% (10%) of the theoretical errors exceeding 0.100 eV (0.150 eV), that is, significantly better than previously reported values. For the prediction of dyes not included in our set, the blind test deviations are ± 14.8 nm (±0.079 eV). In addition, it turns out that the inclusion of f polarization functions in the atomic basis set did not significantly change the transition energies, although sulfur was included in the chromophoric unit, that is, the $\lambda_{\max}$ of thiocarbonyls can be evaluated rapidly, systematically, and efficiently at a proper ab initio level.

For molecules bearing multiple C═S units, the agreement between theory and experiment is also confirmed, though the interpretation of the UV−vis spectra of these dyes likely requires further theoretical and experimental efforts.

Acknowledgment. D.J. and E.A.P. thank the Belgian National Fund for Scientific Research for their research associate positions. The authors are grateful to J. M. André for his continuous support, to M. Bouhy and to C. Lambert for their valuable advices, whereas J. Preat's tremendous humor is always appreciated. Most calculations have been performed on the Interuniversity Scientific Computing Facility (ISCF), installed at the Facultés Universitaires Notre-Dame de la Paix (Namur, Belgium), for which the authors gratefully acknowledge the financial support of the FNRS-FRFC and the "Loterie Nationale" for Convention No. 2.4578.02 and of the FUNDP.

Supporting Information Available: Figures comparing the theoretical and experimental $\Delta E_{\max}$ in electronvolts. This material is available free of charge via the Internet at http://pubs.acs.org.

References and Notes

(1) Zollinger, H. *Color Chemistry, Syntheses, Properties and Applications of Organic Dyes and Pigments*, 3rd ed.; Wiley-VCH: Weinheim, Germany, 2003.

(2) Griffiths, J. *Colour and Constitution of Organic Molecules;* Academic Press: London, 1976.

(3) Jacquemin, D.; Perpète, E. A. *Chem. Phys. Lett.* **2006**, *420*, 529−533.

(4) Maciejewski, A.; Steer, R. P. *Chem. Rev.* **1993**, *93*, 67−98.

(5) Crich, C.; Quintero, L. *Chem. Rev.* **1989**, *89*, 1413−1432.

(6) Janssen, M. J. *Recl. Trav. Chim.* **1960**, *79*, 454−463.

(7) Janssen, M. J. *Recl. Trav. Chim.* **1960**, *79*, 464−473.

(8) Persson, B.; Sandström, J. *Acta Chem. Scand.* **1964**, *18*, 1059−1077.

(9) Sandström, J. *Acta Chem. Scand.* **1962**, *16*, 1616−1626.

(10) Sandström, J. *Acta Chem. Scand.* **1963**, *17*, 678−688.

(11) Sandström, J.; Uppström, B. *Acta Chem. Scand.* **1965**, *19*, 2432−2433.

(12) Berg, U.; Sandström, J. *Acta Chem. Scand.* **1966**, *20*, 689−697.

(13) Korver, O.; Veenland, J. U.; De Boer, T. J. *Recl. Trav. Chim.* **1965**, *84*, 289−303.

(14) Korver, O.; Veenland, J. U.; De Boer, T. J. *Recl. Trav. Chim.* **1965**, *84*, 304−309.

(15) Fabian, J.; Viola, H.; Mayer, R. *Tetrahedron* **1967**, *23*, 4323−4329.

(16) Fabian, J.; Mehlhorn, A. *Z. Chem.* **1967**, *7*, 192−194.

(17) Fabian, J. *Z. Chem.* **1973**, *13*, 26−27.

(18) Judge, T. H.; Moule, D. C.; Bruno, A. E.; Steer, R. P. *Chem. Phys. Lett.* **1983**, *102*, 385−389.

(19) Clouthier, D. J.; Joo, D. L. *J. Chem. Phys.* **1997**, *106*, 7479−7490.

(20) Moule, D. C.; Judge, R. H.; Liu, H.; Lim, E. C. *J. Chem. Phys.* **2000**, *113*, 3937−3940.

(21) He, S. G.; Clouthier, D. J. *J. Chem. Phys.* **2004**, *120*, 8544−8554.

(22) Hirata, S. *J. Chem. Phys.* **2004**, *121*, 51−59.

(23) Labhart, H. *Helv. Chim. Acta* **1957**, *152*, 1410−1421.

(24) Khan, M. S.; Khan, Z. H. *Spectrochim. Acta, Part A* **2003**, *59*, 1409−1426.

(25) Jacquemin, D.; Preat, J.; Wathelet, V.; Perpète, E. A. *J. Chem. Phys.* **2006**, *124*, 074104.

(26) Jacquemin, D.; Preat, J.; Wathelet, V.; Fontaine, M.; Perpète, E. A. *J. Am. Chem. Soc.* **2006**, *128*, 2072−2083.

(27) Downs, A. J. *J. Chem. Soc.* **1962**, 4361−4366.

(28) Adachi, M.; Nakamura, S. *Dyes Pigm.* **1991**, *17*, 287−296.

(29) Runge, E.; Gross, E. K. U. *Phys. Rev. Lett.* **1984**, *52*, 997−1000.

(30) Casida, M. E. In *Accurate Description of Low-Lying Molecular States and Potential Energy Surfaces*; Hoffmann, M. R., Dyall, K. G., Eds.; American Chemical Society: Wahsington, DC, 2002; Vol. 828.

(31) Onida, G.; Reining, L.; Rubio, A. *Rev. Mod. Phys.* **2002**, *74*, 601−659.

(32) Baerends, E. J.; Ricciardi, G.; Rosa, A.; van Gisbergen, S. J. A. *Coord. Chem. Rev.* **2002**, *230*, 5−27.

(33) Maitra, N. T.; Wasserman, A.; Burke, K. In *Electron Correlations and Materials Properties 2*. A. Gonis, N. K., Ciftan, M., Eds.; Kluwer: Dordrecht, The Netherlands, 2003.

(34) Bartholomew, G. P.; Rumi, M.; Pond, S. J. K.; Perry, J. W.; Tretiak, S.; Bazan, G. C. *J. Am. Chem. Soc.* **2004**, *126*, 11529−11542.

(35) Besley, N. A.; Oakley, M. T.; Cowan, A. J.; Hirst, J. D. *J. Am. Chem. Soc.* **2004**, *126*, 13502−13522.

(36) Ciofini, I.; Lainé, P. P.; Bedioui, F.; Adamo, C. *J. Am. Chem. Soc.* **2004**, *126*, 10763−10777.

(37) Improta, R.; Barone, V. *J. Am. Chem. Soc.* **2004**, *126*, 14320−14321.

(38) Rappoport, D.; Furche, F. *J. Am. Chem. Soc.* **2004**, *126*, 1277−1284.

(39) Stich, T. A.; Buan, N. R.; Brunold, T. C. *J. Am. Chem. Soc.* **2004**, *126*, 9735−9749.

(40) Jacquemin, D.; Preat, J.; Wathelet, V.; André, J. M.; Perpète, E. A. *Chem. Phys. Lett.* **2005**, *405*, 429−433.

(41) Chisholm, M. H.; D'Acchioli, J. S.; Pate, B. D.; Patmore, N. J.; Dala, N. S.; Zipse, D. J. *Inorg. Chem.* **2005**, *44*, 1061−1067.

(42) Masternak, A.; Wenska, G.; Milecki, J.; Skalski, B.; Franzen, S. *J. Phys. Chem. A* **2005**, *109*, 759−766.

(43) Jacquemin, D.; Preat, J.; Perpète, E. A. *Chem. Phys. Lett.* **2005**, *410*, 254−259.

(44) Jorge, F. E.; Autschbach, J.; Ziegler, T. *J. Am. Chem. Soc.* **2005**, *127*, 975−985.

(45) Tozer, D. J. *J. Chem. Phys.* **2003**, *119*, 12697−12699.

(46) Dreuw, A.; Head-Gordon, M. *J. Am. Chem. Soc.* **2004**, *126*, 4007−4016.

(47) Burke, K.; Werschnik, J.; Gross, E. K. U. *J. Chem. Phys.* **2005**, *123*, 062206.

(48) Guillaumont, D.; Nakamura, S. *Dyes Pigm.* **2000**, *46*, 85−92.

(49) Fabian, J.; Diaz, L. A.; Seifert, G.; Niehaus, T. *J. Mol. Struct. (THEOCHEM)* **2002**, *594*, 41−53.

(50) Fabian, J. *Theor. Chem. Acc.* **2001**, *106*, 199−217.

(51) Petiau, M.; Fabian, J. *J. Mol. Struct. (THEOCHEM)* **2001**, *538*, 253−260.

(52) Grimme, S.; Izgorodina, E. I. *Chem. Phys.* **2004**, *305*, 223−230.

(53) Furche, F.; Ahlrichs, R. *J. Chem. Phys.* **2002**, *117*, 7433−7447.

(54) Cossi, M.; Barone, V. *J. Chem. Phys.* **2001**, *115*, 4708−4717.

(55) Hommen de Mello, P.; Mennucci, B.; Tomasi, J.; da Silva, A. B. F. *Theor. Chem. Acc.* **2005**, *113*, 274−280.

(56) Frisch, M. J.; et al. *Gaussian 03*, revision B.04; Gaussian, Inc.: Wallingford, CT, 2004.

(57) Becke, A. D. *J. Chem. Phys.* **1993**, *98*, 5648−5652.

(58) Becke, A. D. *Phys. Rev. A* **1988**, *38*, 3098−3100.

(59) Lee, C.; Yang, W.; Parr, R. G. *Phys. Rev. B* **1988**, *37*, 785−789.

(60) Adamo, C.; Barone, V. *J. Chem. Phys.* **1999**, *110*, 6158−6170.

(61) Ernzerhof, M.; Scuseria, G. E. *J. Chem. Phys.* **1999**, *110*, 5029−5036.

(62) Perdew, J. P.; Burke, K.; Ernzerhof, M. *Phys. Rev. Lett.* **1996**, *77*, 3865−3868.

(63) Perdew, J. P.; Ernzerhof, M.; Burke, K. *J. Chem. Phys.* **1996**, *105*, 9982−9985.

(64) Teixeira-Dias, J. J. C.; Jardim-Barreto, V. M.; Ozaki, Y.; Storer, A. C.; Carey, P. R. *Can. J. Chem.* **1982**, *60*, 174−189.

(65) Tomasi, J.; Mennucci, B.; Cammi, R. *Chem. Rev.* **2005**, *105*, 2999−3094.

(66) *Statgraphics Plus 5.1*; Manugistics Inc.: Herndon, VA, 2000.

(67) Barrett, J.; Deghaidy, F. S. *Spectrochim. Acta, Part A* **1975**, *31*, 707−713.

(68) Perpète, E. A.; Wathelet, V.; Preat, J.; Lambert, C.; Jacquemin, D. *J. Chem. Theor. Comput.* **2006**, *2*, 434−440.

(69) Simard, B.; Hackett, P. A.; Steer, R. P. *J. Mol. Spectrosc.* **1987**, *126*, 307−328.

(70) Fabian, J.; Mayer, R. *Spectrochim. Acta* **1964**, *20*, 299−304.

(71) Barbarella, G.; Bongini, A.; Rossini, S. *J. Org. Chem.* **1988**, *53*, 5140−5142.

(72) Giles, H. G.; Marty, R. a.; De Mayo, P. *Can. J. Chem.* **1976**, *54*, 537−542.

(73) Middleton, W. J.; Howard, E. G.; Sharkey, W. H. *J. Org. Chem.* **1965**, *30*, 1375−1384.

(74) Brown, H. C.; Pater, R. *J. Org. Chem.* **1962**, *27*, 2858−2863.

(75) Simmons, H. E.; Blomstrom, D. C.; Vest, R. D. *J. Am. Chem. Soc.* **1962**, *84*, 4756−4771.

(76) Ramnath, N.; Ramesh, V.; Ramamurthy, V. *J. Org. Chem.* **1983**, *48*, 214−222.

(77) De Mayo, P.; Weedon, A. C.; Wong, G. S. K. *J. Org. Chem.* **1979**, *44*, 1977−1981.

(78) Metzner, P.; Vialler, J. *Bull. Soc. Chim. Fr.* **1972**, 3138−3145.

(79) Machiguchi, T.; Otani, H.; Ishii, Y.; Hasegawa, T. *Tetrahedron Lett.* **1987**, *28*, 203−206.

(80) Elam, E. U.; Davis, H. E. *J. Org. Chem.* **1967**, *32*, 1562−1565.

(81) Krebs, A.; Rüger, W.; Ziegenhagen, B.; Hebold, M.; Hardtke, I.; Müller, R.; Schütz, M.; Wietzke, M.; Wilke, M. *Chem. Ber.* **1984**, *117*, 277−309.

(82) Elam, E. U.; Rash, F. H.; Dougherty, J. T.; Goodlett, V. W.; Brannock, K. C. *J. Org. Chem.* **1968**, *33*, 2738−2741.

(83) Raasch, M. S. *J. Org. Chem.* **1970**, *35*, 3470−3483.

(84) Pushkara Rao, V.; Rammamurthy, V. *J. Org. Chem.* **1988**, *53*, 332−339.

(85) Raasch, M. S. *J. Org. Chem.* **1979**, *44*, 632−633.